Journal of Solid State Chemistry **146,** 266–270 (1999)
Article ID jssc.1999.8352, available online at http://www.idealibrary.com on IDEAL®

Neutron Diffraction Study of the Crystal Structure of $BaMoO_4$: A Suitable Precursor for Metallic $BaMoO_3$ Perovskite

Vivian Nassif and Raúl E. Carbonio

Instituto de Investigaciones en Fisicoquímica de Córdoba (INFIQC), Departamento de Físico Química, Facultad de Ciencias Químicas, Universidad Nacional de Córdoba, Ciudad Universitaria, 5000 Córdobo, Argentina

and

José A. Alonso[1]

Instituto de Ciencia de Materiales de Madrid, C.S.I.C., Cantoblanco, 28049 Madrid, Spain

Received February 1, 1999; accepted April 22, 1999

$BaMoO_3$, metallic and Pauli paramagnetic, has been prepared by controlled reduction of $BaMoO_4$. This precursor, containing Mo(VI), is unusually stable against reduction, due to structural factors. The crystal structure of $BaMoO_4$ has been refined from neutron powder diffraction data: space group $I4_1/a$ (no. 88), $Z = 4$, $a = 5.5479(9)$, and $c = 12.743(2)$ Å. A bond-valence study allowed us to detect the presence of slight tensile and compressive stresses in the crystal structure of $BaMoO_4$, in which Ba is overbonded and Mo is underbonded. However, this effect is less pronounced than in other AMO_4 oxides with a scheelite structure (A = Ca, Sr, Ba; M = Mo, W): $BaMoO_4$ contains the M cation exhibiting the closest valence to the nominal value of 6+, suggesting a large covalent contribution to the Mo–O bonds. This observation is coherent with the large thermal stability of this compound against reduction, taking place at temperatures above 920°C in H_2 flow.

Key Words: **neutron powder diffraction; crystal structure; thermal analysis.**

INTRODUCTION

Twenty years ago, Goodenough established a scheme and gave a criterion for localized vs collective *d*-electron behaviors in transition-metal oxides, ABO_3, with a perovskite structure (1, 2). According to this criterion, $AMoO_3$ (A = Ca, Sr, Ba) have so sufficient electron-transfer energies as to screen and cancel the electrostatic energy accompanied by the electron transfer. Thus, $AMoO_3$ can be classified into the superconducting possible materials. The low-temperature electronic conductivities of these compounds have been studied in the past: $BaMoO_3$ and $SrMoO_3$ are cubic perovskites showing metallic conductivity and Pauli paramagnetism (3–5).

In our current research on the electronic properties of Vb and VIb transition-metal oxides in intermediate oxidation states (e.g., Nb(IV), Mo(IV)), we are interested in the preparation and study of hole and electron-doped compounds, $Ba_{1-x}A_xMoO_3$ (e.g., A^{3+} = La; A^{+} = K). As a preliminary study, we prepared $BaMoO_3$ as a reduction product of $BaMoO_4$. The thermal stability under reducing conditions of this precursor containing Mo(IV) is surprisingly high (6): it only takes place at O_2 pressures below $\log P(O_2) = -13.7$ at 1200°C. The microscopic origin of the observed high stability was uncertain, due to the lack of precise structural information on the precursor material, barium molibdate, $BaMoO_4$.

It is well known that $BaMoO_4$ adopts a scheelite-like structure (7). In the scheelite structure, AMO_4, which can be considered as a superstructure of CaF_2 flourite, the two kinds of metal atoms are ordered along the **c** axis of the tetragonal unit cell. The crystal structure is typified by $CaWO_4$ and can be described in the space group $I4_1/a$ (no. 88). Both metal atoms are placed at special positions, whereas O anions are at general positions, $16f(x, y, z)$. Most of the isostructural AMO_4 ternary oxides (A = Ca, Sr, Ba; M = Mo, W), except $BaMoO_4$, have been structurally refined from neutron diffraction data, allowing the precise determination of oxygen positions [8–10]. The most recent determination (11) of $BaMoO_4$, from 1970, is basically incorrect.

The lack of good structural data for $BaMoO_4$ led us to undertake a neutron diffraction study of this compound and to establish a comparison with other related molibdates and

[1] To whom correspondence should be addressed. Fax: 34 91 372 0623. E-mail: ja.alonso@icmm.csic.esI.

PACS numbers: 61.12Ld, 61.66.Fn, 74.10 + V.

0022-4596/99 $30.00

tungstates. The reduction process to give metallic $BaMoO_3$, studied by TG techniques, is also reported.

EXPERIMENTAL

White polycrystalline $BaMoO_4$ was prepared according to the following reaction:

$$(NH_4)_2MoO_4(aq) + BaCl_2(aq) \xrightarrow{NH_4OH(aq, pH = 10)} BaMoO_4(s) + 2(NH_4)Cl(aq). \quad [1]$$

Aqueous solutions of analytical grade $BaCl_2$ and $(NH_4)_2MoO_4$, 1 M each, were prepared separately. NH_4OH was added to the molibdate solution, to reach pH = 10. $BaCl_2$ solution was poured slowly with constant stirring into the $(NH_4)_2MoO_4$ solution. The precipitate was digested for 48 h at 60°C in the mother solution, to improve its crystallinity. The resultant precipitate was filtered, washed thoroughly with distilled water, and dried in a vacuum oven at 110°C and then in an oven at 600°C in air for 24 h. $BaMoO_3$ was prepared as a dark red colored powder by heating $BaMoO_4$ at 1150°C in an H_2/N_2 (5%:95%) flow, for 12 h. The reduction process was followed by thermal analysis using a Mettler TA3000 system equipped with a TC10 processor unit. Thermogravimetric (TG) curves were obtained in a TG50 unit, working at a heating rate of 5°C min^{-1}, in a reducing H_2 flow of 0.3 l min^{-1}. About 50 mg of the sample was used in the experiment.

The products ($BaMoO_4$, $BaMoO_3$) were characterized by X-ray diffraction (XRD) using Cu$K\alpha$ radiation, in a Siemens D-501 goniometer controlled by a DACO-MP computer, by step scanning from 10 to 100° in 2θ, in increments of 0.05° and a counting time of 4 s each step.

The neutron powder diffraction (NPD) pattern of $BaMoO_4$ was collected at room temperature in the multidetector DN5 diffractometer at the Siloé reactor of the Centre d'Etudes Nucléaires, Grenoble. A wavelength of 1.345 Å was selected from a Cu monochromator. The 800 detectors covered a 2θ range of 80°, from $2\theta_i = 12°$. The counting time was about 4 h, using 10 g of sample contained in a vanadium can.

NPD and XRD patterns were analyzed by the Rietveld (12) method, using the FULLPROF program (13). The lineshape of the diffraction peaks was generated by a pseudo-Voigt function and the background refined to a fifth-degree polynomial. In the neutron refinement, the coherent scattering lengths for Ba, Mo, and O were, respectively, 5.07, 6.72, and 5.805 fm. In the final run, the following parameters were refined: background coefficients, zero-point, half-width, pseudo-Voigt, and asymmetry parameters for the peak shape; scale factor, positional, thermal isotropic factors for Ba and anisotropic for Mo and O, and unit-cell parameters.

RESULTS AND DISCUSSION

Thermal Analysis under Reducing Conditions of $BaMoO_4$

The thermal behavior of $BaMoO_4$ in a reducing H_2 flow is illustrated in Fig. 1. The sample is stable up to 920°C; beyond this temperature, the TG curve shows a reduction process, which can be completed by isothermal heatings above 1000°C. After this process, $BaMoO_3$ can be identified as a major reduction product by XRD. The observed weight loss for this reduction agrees with the calculated weight loss for the equation

$$BaMoO_4 + H_2 \rightarrow BaMoO_3 + H_2O. \quad [2]$$

Structural Study

$BaMoO_4$ and $BaMoO_3$ were obtained as well-crystallized powders, whose XRD diagrams are characteristic of sheelite and perovskite structures, respectively. Figure 2 shows the indexed XRD diagrams for both compounds. The structural refinement from NPD data of $BaMoO_4$ was performed by the Rietveld method, taking as the starting parameters those of $BaWO_4$ (9). The final atomic coordinates, unit-cell parameters, and discrepancy factors after the refinement are included in Table 1. Figure 3 shows the good agreement between observed and calculated NPD profiles for $BaMoO_4$.

The XRD pattern of $BaMoO_3$ was refined in a simple cubic perovskite unit cell, with edge **a** = 4.0448(2) Å and all the atoms placed at special positions. Since small amounts of Mo Metal and unreacted $BaMoO_4$ were detected as impurity phases, they were included in a final multiphase

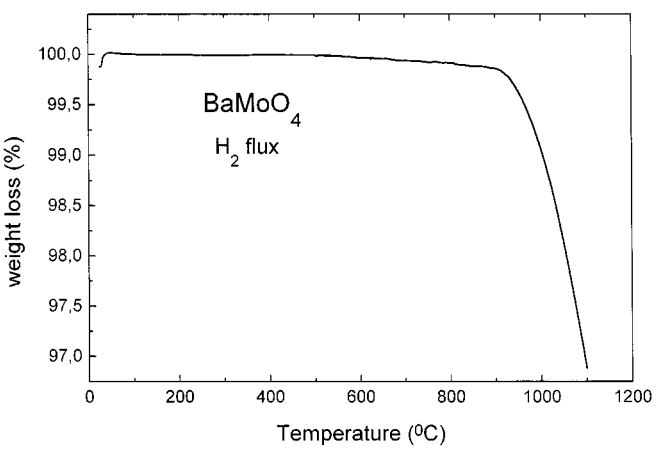

FIG. 1. TG curve for $BaMoO_4$, obtained in a reducing H_2 flow. The complete reduction to give $BaMoO_3$ corresponds to a weight loss of 5.38%.

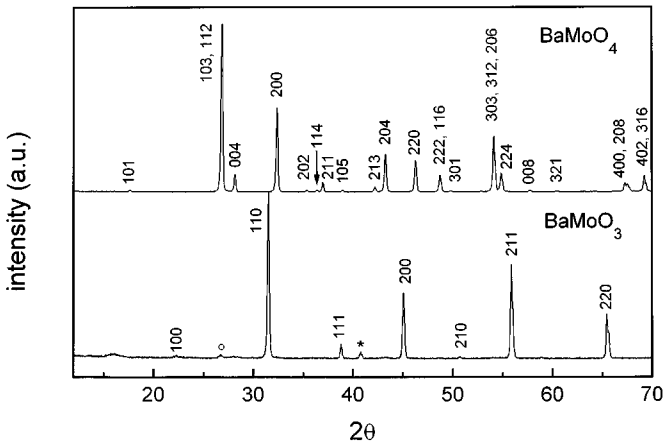

FIG. 2. XDR patterns of (a) $BaMoO_4$, indexed on the basis of a tetragonal unit cell with **a** = 5.5479(9) and **c** = 12.743(2) Å, and (b) $BaMoO_3$, cubic with **a** = 4.0448(2) Å.

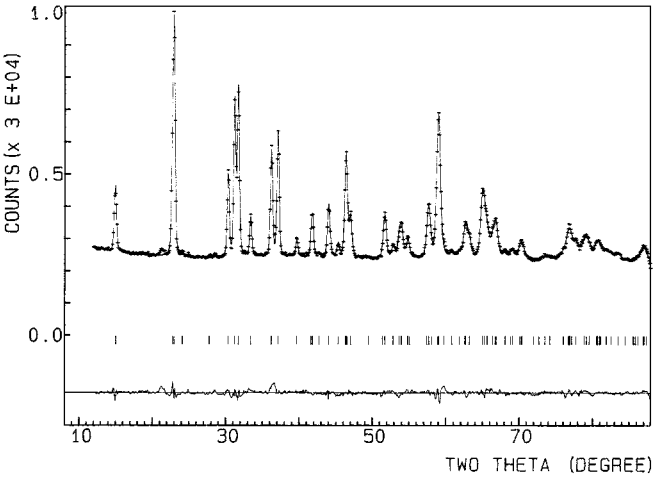

FIG. 3. Observed (crosses), calculated (solid line), and difference (at the bottom) neutron diffraction profiles for $BaMoO_4$ at 295 K. The tick marks indicate the positions of the allowed Bragg reflections.

refinement. No additional superstructure reflections or splitting of the peaks were detected, excluding the departure of the $Pm\bar{3}m$ symmetry. Figure 4 shows the goodness of the fit for $BaMoO_3$ XRD profiles.

Table 2 contains a selected list of distances and angles for $BaMoO_4$, and a view of the structure is shown in Fig. 5. Ba^{2+} cations are coordinated to eight oxygens placed in the corners of distorted cubes, better described as scalenohedra. The oxygen coordination polyhedra of Mo^{6+} cations are slightly distorted tetrahedra, showing O–Mo–O angles of 108.3 and 111.8°.

The valence of the cations and anions present in the solid can be estimated by means of the Brown's bond valence model (14, 15). This model gives a phenomenological relationship between the formal valence of a bond and the corresponding bond length. In perfect nonstrained structures, the bond valence sum (BVS) rule states that the formal charge of the cation (anion) is equal to the sum of the bond valences around this cation (anion). This rule is satisfied only if the stress introduced by the coexistence of different structural units can be relieved by the existence of enough degrees of freedom in the crystallographic structure. The departure of the BVS rule is a measure of the existing stress in the bonds of the structure.

Table 3 lists the valences calculated for Ba, Mo, and O from the individual Ba–O and Mo–O distances of Table 2 for $BaMoO_4$. The valence of the Ba cation is slightly higher than the expected value of +2; in compensation, the valence of Mo atom is slightly lower than +6. This result suggests that Ba atoms are overbonded while Mo are underbonded in this structure; in other words, Ba–O bonds are,

TABLE 1

Crystallographic Parameters for $BaMoO_4$, after the Profile Refinement of NPD Data at 295 K (Space Group $I4_1/a$ (No. 88), $Z = 4$, a = 5.5479(9), and c = 12.743(2) Å)

Atom	Site	x	y	z	B_{eq} (Å)
Ba	4*b*	0	$\frac{1}{4}$	$\frac{5}{8}$	0.27(9)
Mo	4*a*	0	$\frac{1}{4}$	$\frac{1}{8}$	0.90(9)[a]
O	16*f*	0.2362(5)	0.1331(4)	0.0473(2)	1.12(6)[a]

Note. R factors: $R_p = 1.60$, $R_{wp} = 2.15$, $R_{exp} = 1.04\%$, $X^2 = 4.24$, and $R_I = 3.50\%$.

[a] Anisotropic thermal factors: for Mo, $\beta_{11} = \beta_{22} = 0.0099(6)$, and $\beta_{33} = 0.0015(2)$; for O, $\beta_{11} = 0.0163(6)$, $\beta_{22} = 0.0076(5)$, $\beta_{33} = 0.0013(1)$, $\beta_{12} = 0.012(1)$, $\beta_{13} = 0.0006(3)$, and $\beta_{23} = 0.0013(4)$.

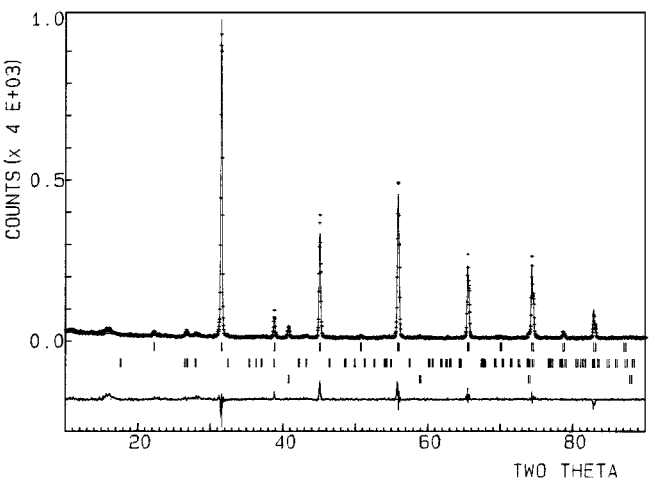

FIG. 4. Observed, calculated, and difference XRD profiles for $BaMoO_3$. The second and third series of tick marks correspond to minor $BaMoO_4$ and Mo impurity phases.

TABLE 2
Selected Interatomic Distances (Å) and Angles (°) in $BaMoO_4$

		BaO_8 scalenohedron		
Ba–O	×4	2.764(3)	O–Ba–O	75.5(1)
Ba–O	×4	2.718(3)	O–Ba–O	72.2(1)
			O–Ba–O	67.0(1)
			O–Ba–O	79.2(1)
			O–Ba–O	146.1(2)
			O–Ba–O	130.8(2)
			O–Ba–O	138.0(2)
			O–Ba–O	97.4(1)
		MoO_4 tetrahedron		
Mo–O	×4	1.765(3)	O–Mo–O	111.8(2)
			O–Mo–O	108.3(2)

TABLE 3
Bond Valences (s_i) for Ba–O and Mo–O Bonds, Multiplicity of the Bonds [m], and Valences ($\sum s_i$) for Ba, Mo, and O Atoms within the Respective Coordination Polyhedra in the $BaMoO_4$ Structure

Atom	s_i, [m]	$\sum s_i$
Ba	0.278(2), [4] 0.315(2), [4]	2.372(6)
Mo	1.47(1), [4]	5.88(2)
O	0.278(2), [1] 0.315(2), [1] 1.47(1), [1]	2.06(1)

Note. The valence is the sum of the individual bond valences (s_i) for Ba–O and Mo–O bonds. Bond valences are calculated as $s_i = \exp[(r_0 - r_i)/B]$; $B = 0.37$; $r_0(\mathrm{Ba}) = 2.29$, $r_0(\mathrm{Mo}) = 1.907$ Å for the Ba^{2+}–O^{2-} and Mo^{6+}–O^{2-} pairs, respectively (from Ref. (15)). Individual Ba–O and Mo–O distances are taken from Table 2.

on average, under compressive stress and Mo–O bonds are under tensile stress, giving rise to a structure with a slight metastable character. The large thermal factor of Mo ($B_{eq} = 0.90(9)$ Å^2) compared with that of Ba (0.27(9) Å^2) seems to be related to the underbonded character of the former.

It is interesting to compare $BaMoO_4$ with other related oxides with a scheelite structure, AMO_4, where A = Ca, Sr, Ba and M = W, Mo, from the point of view of the cation valences in the corresponding oxygen coordination polyhedra. In Table 4, the common feature for all of the studied oxides is the underbonded character of M cations. However, it is striking to note that $BaMoO_4$ is the oxide in which the transition-metal cation exhibits the closest valence to the expected value of 6+.

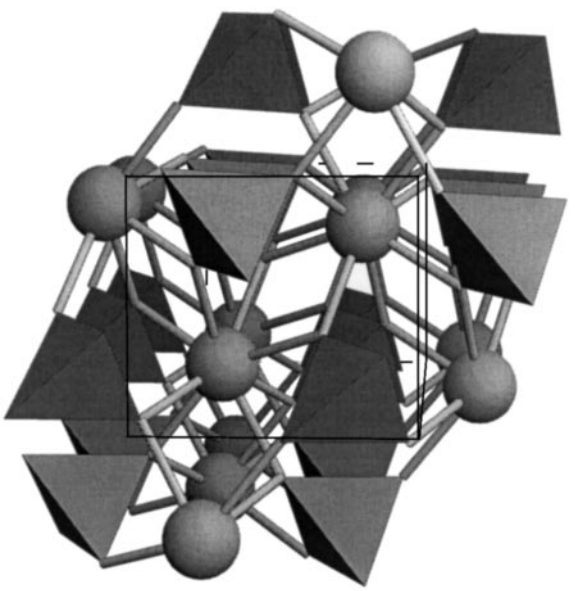

FIG. 5. View of the $BaMoO_4$ structure, along the [100] direction, with **c** axis vertical. Tetrahedra correspond to MoO_4 units. Large spheres are Ba^{2+} cations. The coordination of peripheral Ba^{2+} cations is incomplete.

In the $A\mathrm{MoO}_4$ series (A = Ca, Sr, Ba) this fact can be understood, taking into account the contribution of covalent bonding to the strength of Mo–O bonds: A and Mo cations compete against each other for the electron cloud of O^{2-} through their Coulombic potential Ze^2/r (Z, valence; r, ionic radius); A^{2+} cations with a lower Coulombic potential enables an increase the overlap of electron clouds between Mo and O ions, giving rise to a stronger covalent bonding: the highest valence is expected in the ternary oxide with the largest A^{2+} cation, in this case Ba^{2+}.

For a given A^{2+} cation, Mo–O distances are systematically shorter than W–O bond lengths, corresponding to the smaller ionic size of Mo cations in the nominal oxidation state of 6+ (Shannon's (16) ionic radii: Mo^{6+}, 0.41 Å; W^{6+}, 0.42 Å, in tetrahedral coordination). The higher valence of Mo compounds is also related to the stronger Coulombic potential of Mo^{6+} cations with respect to larger W^{6+} ions, giving rise in the former case to stronger covalent bondings to oxygen.

TABLE 4
Valences ($\sum s_i$) Determined from the Bond Valence Model for A, M, and O within the AO_8 and MO_4 Coordination Polyhedra in AMO_4 Oxides with a Scheelite Structure (A = Ca, Sr, Ba; M = Mo, W)

AMO_4	$CaWO_4$	$CaMoO_4$	$SrWO_4$	$SrMoO_4$	$BaWO_4$	$BaMoO_4$
Ref.	(9)	(9)	(8)	(8)	(8)	This work
A–O (×4)	2.478(5)	2.465(3)	2.610(3)	2.610(4)	2.778(3)	2.764(3)
A–O (×4)	2.441(5)	2.451(3)	2.580(3)	2.583(4)	2.738(3)	2.717(3)
M–O (×4)	1.782(5)	1.771(3)	1.779(3)	1.767(4)	1.782(3)	1.765(3)
$\sum s_i(A)$	2.12(1)	2.122(7)	2.208(5)	2.194(9)	2.261(6)	2.372(6)
$\sum s_i(M)$	5.77(4)	5.78(3)	5.81(2)	5.84(3)	5.76(2)	5.88(2)
$\sum s_i(\mathrm{O})$	1.97(2)	1.98(1)	2.01(1)	2.01(2)	2.01(1)	2.06(1)

Note. r_0 values for Ca^{2+}, Sr^{2+}, and W^{6+} are, respectively, 1.967, 2.118, and 1.921 from Ref. (15).

This picture, in which the observed valence of M cations leads to a relative estimate of the strength of the covalent bondings in the MO_6 polyhedra, is complementary to the results reported by Kamata *et al.* (6) about the thermal stability of the series of alkaline-earth molibdates, $AMoO_4$: the high valence state of Mo in these ternary oxides becomes more durable against reduction as the A^{2+} radius is larger. In the present work, a precise determination of the oxygen structural parameters for $BaMoO_4$ from NPD data allowed us to understand the microscopic origin of this behavior.

CONCLUSIONS

Neutron diffraction data reveal that although Mo(VI) cations are slightly underbonded in the $BaMoO_4$ crystal structure, they form stronger covalent bondings to oxygen than any of the isostructural AMO_4 oxides (A = Ca, Sr, Ba; M = Mo, W). This finding explains the large thermal stability against reduction of $BaMoO_4$, also more stable than other $AMoO_4$ oxides with a scheelite structure. Thermal analysis in H_2 flow shows that the reduction process to give the cubic perovskite $BaMoO_3$, containing Mo(IV), takes place at temperatures above 920°C.

ACKNOWLEDGMENTS

The authors acknowledge the financial support of the DGICYT to the Project PB97-1181 and the spanish Ministerio of Educacion y Cultura for funds to a Proyecto de Cooperación Iberoamericana. They also thank the MDN group at the CEN–Grenoble for their hospitality and for the facilities at the Siloé reactor. R.E.C. thanks Fundación Antorchas, SECYT-UNC, CONICOR, ANPCYT, and CONICET for research grants.

REFERENCES

1. J. B. Goodenough, *J. Appl. Phys.* **37,** 1415 (1966).
2. J. B. Goodenough and J. M. Longo, *Landolt-Borstein Zahlenwerte und Funktionen, New Series* **BdIII/4a,** 255 (1970).
3. L. H. Brixner, *J. Inorg. Nucl. Chem.* **14,** 225 (1960).
4. G. H. Bouchard and M. J. Sienko, *Inorg. Chem.* **7,** 441 (1968).
5. S. Hayashi, R. Aoki, and T. Nakamura, *Mater. Res. Bull.* **14,** 409 (1979).
6. K. Kamata, T. Nakamura, and T. Sata, *Mater. Res. Bull.* **10,** 373 (1975).
7. F. Galasso, *in* "Structure and Properties of Inorganic Solids." p. 106. Pergamon Press, Oxford, (1970).
8. E. Guermen, E. Daniels, and J. S. King, *J. Chem. Phys.* **55,** 1093 (1971).
9. R. M. Hazen, L. W. Finger, and J. W. E. Mariathasan, *J. Phys.* **46,** 253 (1985).
10. G. Wandal and A. Norlund-Christensen, *Acta Chem. Scand.* **41,** 358 (1987).
11. T. I. Bylichkina, L. I. Soleva, E. A. Pobedimskaya, M. A. Porai-Koshits, and N. V. Belov, *Kristallografiya* **15,** 165 (1970).
12. H. M. Rietveld, *J. Appl. Crystallogr.* **2,** 65 (1969).
13. J. Rodríguez-Carvajal, *Physica B* **192,** 55 (1993).
14. I. D. Brown, *in* "Structure and Bonding in Crystals," (M. O'Keefe and A. Navrotsky, Eds.), Vol. 2, p. 1. Academic Press, New York, 1981.
15. N. E. Brese and M. O'Keefe, *Acta Crystallogr., Sect. B* **47,** 192 (1991).
16. R. D. Shannon, *Acta Crystallogr., Sect. A* **32,** 751 (1976).